

Supporting information

Fine-tuned H-ferritin nanocage with multiple gold clusters as near-infrared kidney specific-targeting nanoprobe

Cuiji Sun, Yi Yuan[‡], Zhonghe Xu, Tianjiao Ji, Yanhua Tian, Shan Wu, Jianlin Lei, Jingyuan Li^{}, Ning Gao^{*}, Guangjun Nie^{*}*

Table of contents

Methods

Figure S1

Figure S2

Figure S3

References

Methods

HFt expression and purification. Human HFt recombinant plasmid was transformed into *E. coli* expression strain BL21 (DE3). Protein was over expressed in LB medium by induction of 0.5 mM IPTG (isopropyl- β -D-thiogalactopyranoside) at 37°C, for 4 h. Cells were harvested by centrifugation, and resuspended in 40 mL of lysis buffer (20 mM Tris-HCl, pH 8.0, 50 mM NaCl, 1 mM PMSF) and lysed by sonication. The supernatant was incubated at 60°C for 15min to precipitate the thermolabile proteins of *E.coli*. The supernatant was further purified by gel filtration column (Superdex 200, GE Healthcare). Fractions were examined by SDS-PAGE. Purified HFt was concentrated and stored at -80°C. All the purification experiments were performed in 4°C. HFt subunits self-assembled into 24mer nanocages and the overall morphology of the cage was confirmed by Cryo-EM.

Preparation of NIR Au-HFt. HAuCl₄ (0.781 mL; 20 mM, pH 7) was added to 5 mL HFt (5 mg/mL). After shaking and mixing for 2 min, 1M NaOH was added to change the pH of the solution to 11, followed by incubation at 37°C for 72 h. After the NIR Au-HFt was formed, the reaction solution was filtered with a centrifugal filter device (Amicon Ultra-15; 30,000 molecular weight cut-off) and washed three times with 3 mL double distilled water. The concentration of HFt protein was measured by the bicinchoninic acid method (BCA).

The quantum yield of Au-HFt. The quantum yield (QY) of Au-HFt was determined by measuring the integrated fluorescence intensities of the Au-HFt and the reference compound (HITCI in basic ethanol, QY = 28.3%) under 722 nm excitation with LS55fluorescence spectrometry¹.

Cryo-EM. Cryo-grids were prepared with Quantifoil2/2 holey carbon grids (Quantifoil Micro Tools GmbH). An aliquot of 4 μ L of diluted sample of Au-HFt (approximately 15 mg/ml) was blotted inside an FEI Vitrobot Mark IV at 4°C, vitrified into liquid ethane and stored in liquid nitrogen. Cryo-samples were examined at liquid nitrogen temperature in an FEI F20 operated at 200 kV using a nominal magnification of 80,000 \times . Images were recorded on a Gatan 4k \times 4k CCD camera under low-dose condition with a dose of approximately 25e-/Å². The effective pixel size on the object scale is 2.9 Å.

High resolution transmission electron microscopy. An aliquot of 4 μ L far-red Au-HFt (360 nM) was applied to a glow-discharged grid coated with a layer of amorphous carbon film and excess fluid was gently blotted off with filter paper. The HRTEM images were recorded on an FEI TecnaiF20 U-TWIN electron microscope.

In vivo and ex vivo imaging with NIR Au-HFt. Nu/nu female mice (8 weeks, 20 \pm 2g) obtained from Beijing Vital River Laboratories were injected via the tail vein with the Au-HFt probe (0.2 nmol/g body weight) diluted in 0.9% NaCl solution. In vivo fluorescence images of the mice were obtained with a MaestroTM in vivo spectrum imaging system (Cambridge Research & Instrumentation,

Woburn, MA, USA). The excitation filter was set as 650 to 750 nm; the emission filter was a 635 nm long-pass filter. The liquid crystal tunable emission filter (LCTF, with a bandwidth of 20 nm and a scanning wavelength range of 500 to 950 nm) was automatically stepped in 10 nm increments from 720 to 860 nm while the CCD captured images at each wavelength with constant exposure. At the special time points of 0.5, 1, 1.5, 4 h after injection, the mice were sacrificed and the organs were removed for ex vivo fluorescence imaging on the same spectrum imaging system. All animal experiments were approved by the Animal Ethics Committee of the Medical School, Beijing University.

ICP-MS. NIR Au-HFt tissue distribution was assessed by measuring Au levels by ICP-MS (Elemental X7, Thermo Electron). Tissues were removed, washed and weighted. For each sample, 10-30 mg of tissue was digested in nitric acid and heated at 120°C for several hours. Hydrogen peroxide solution was used to drive off the vapor of nitrogen oxides until the solution was colorless and clear. After the solution volume was adjusted to 2 mL using 2% nitric acid and 1% hydrochloride acid, the Au content was analyzed using ICP-MS. Indium (20 ng/mL) was used as an internal standard.

Molecular dynamics simulation. The crystal structure of human ferritin heavy chain (HFt subunit) was obtained from the protein data bank (3AJ0). The hexamer comprised of six subunits (three dimers) was constructed, corresponding to half of ferritin equator (also see Figure 1d). The hexamer was then solvated by SPCE water model, and the dimension of simulation system is $161 \times 130 \times 92 \text{ \AA}^3$. Counter-ions were added to neutralize the system. Initial concentration of gold atoms is 0.1 M. During the growth of gold cluster on the hexamer of HFt subunits, the effective concentration in the solution decreases. Additional gold atoms were then added to the solution to maintain the concentration of free gold atoms. The simulation was performed at constant temperature (300K) and pressure (1 atm) using GROMACS package 4.6.1.² And the temperature and pressure were controlled by Velocity Scaling and Berendsen methods, respectively. Gromos53a6 force field³ was used to describe the interaction of protein, and the interaction of gold atom was described by CVFF force field.⁴ The cutoff distance for the calculations of both van der Waals interaction and short-range electrostatic interaction was 10 Å. The long range electrostatic interactions were handled by the particle-mesh Ewald (PME) method. The snapshots were visualized with VMD package 1.9.1.⁵

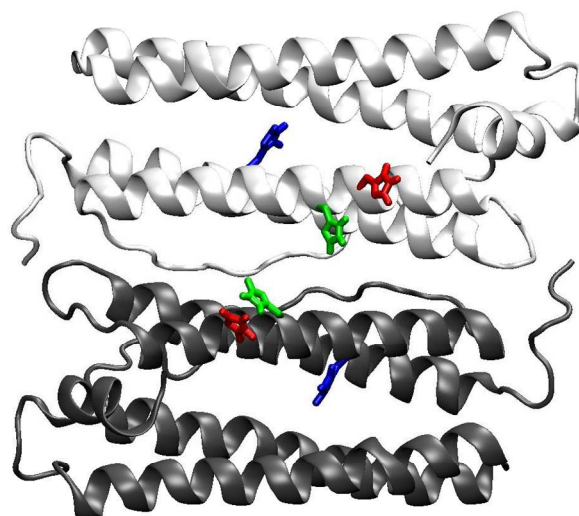


Figure S1. Subunit homodimer of HfT subunit is shown in cartoon representation, with HIS residues in putative growth site shown in stick models. His57, His60 and His65 are displayed in red, green and blue, respectively.

Molecular dynamics (MD) simulation was conducted to investigate the Au cluster on the inner surface of ferritin. It has been well accepted that the Au atoms can strongly bound to His residues. And we noticed that there are three His residues, His57, His60 and His65, distribute on the inner surface of subunit and close to each other, especially His57 and His60 (Figure S1). On top of this, the distance between the residues belong to two subunits in a dimer is small. Compared to His65, the imidazole rings of His57 and His60 are even more exposed (with larger solvent accessible surface area, SASA). We found the gold atoms tend to bind to these two residues. The formation and growth of gold cluster were observed in the putative growth sites of all three dimers (Figure S2). For each dimer, the Au cluster can form in each subunit separately. As the growth of Au cluster, these two clusters can eventually merge.

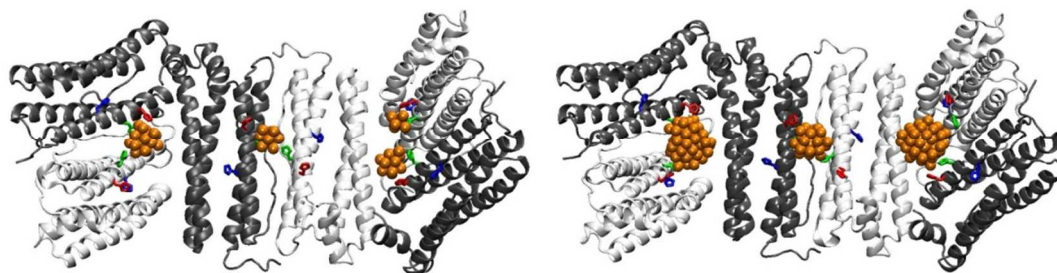


Figure S2. Snapshot of subunit hexamer and gold clusters at $t = 160$ ns (left) and 320 ns (right). The monomers in each dimer are colored light and dark gray separately, and His57, His60 and His65 are displayed in red, green and blue respectively.

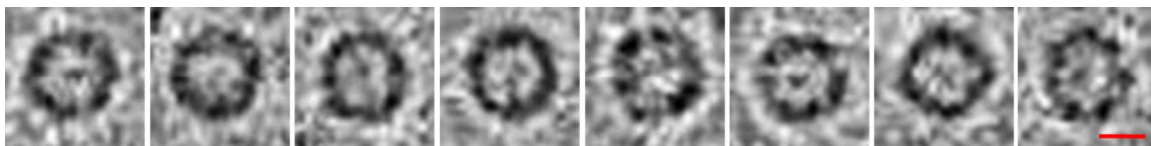


Figure S3. Au-HfT particles picked from the Cryo-EM map. Darker contrast dots on the spherical shell represent multiple gold clusters. The scale bar is 5 nm.

References for supporting information

- (1) Rurack, K.; Speles, M. *Anal.Chem.* **2011**, *83*, 1232.
- (2) Lawson, D. M.; Artymiuk, P. J.; Yewdall, S. J.; Smith, J. M.; Livingstone, J. C.; Treffry, A.; Luzzago, A.; Levi, S.; Arosio, P.; Cesareni, G. *Nature* **1991**, *349*, 541.
- (3) Oostenbrink, C.; Villa, A.; Mark, A. E.; Van Gunsteren, W. F. *Comp. Chem.* **2004**, *25*, 1656.
- (4) Heinz, H.; Vaia, R.; Farmer, B.; Naik, R. *J. Phy. Chem. C* **2008**, *112*, 17281.
- (5) Humphrey, W.; Dalke, A.; Schulten, K. *Mole.Graph.* **1996**, *14*, 33.